ORIGINAL RESEARCH

Dye adsorption performance of nanocellulose beads with different carboxyl group content

**Jianghua Xue · Enwen Zhu · Hengfeng Zhu ·
Dongning Liu · Haopeng Cai · Chuanxi Xiong ·
Quanling Yang · Zhuqun Shi**

Abstract The problems caused by water pollution are increasingly serious, wastewater contains a lot of heavy metal ions, textile dyes, medicines, etc. However, most adsorption materials usually face problems such as inefficient recycling, high cost, and secondary pollution. As a natural polymer, cellulose has low cost, degradability and good biocompatibility. In this work, by changing the addition amount of sodium hypochlorite during 2,2,6,6-Tetramethylpiperidine-1-oxyl radical (TEMPO) oxidation, nanocellulose with different carboxyl content could be prepared, which is expected to be a good high-efficiency cationic adsorbent due to its rich in hydroxyl groups on the surface and negatively charged. Then the calcium chloride solution was used as the cross-linking agent to prepare TEMPO-oxidized cellulose nanofibril beads (TOCNB) by the dropping solidification method. As the content of carboxyl groups increases, the Zeta potential value of the nanocellulose dispersion became increasingly negative. The nanocellulose beads all presented a good three-dimensional network porous structure. With the increase of carboxyl group content, the specific surface area increases from 173 to 367 $m^2 g^{-1}$, and the adsorption capacity for methylene blue (MB) also gradually strengthened. The saturated adsorption capacity of TOCNB on MB was calculated as high as 925.93 $mg g^{-1}$. The nanocellulose bead was a cationic adsorbent with highly efficient adsorption and adjustable specific surface area, and the preparation method was simple, fast, efficient and green.

Keywords Nanocellulose beads · Dye adsorption · Methylene blue · Carboxyl content

Jianghua Xue and Enwen Zhu have contributed equally to this work.

J. Xue · E. Zhu · H. Zhu · D. Liu · H. Cai (✉) · C. Xiong · Q. Yang (✉) · Z. Shi (✉)
School of Materials Science and Engineering, Wuhan University of Technology, Wuhan 430070, China
e-mail: cai_haopeng@whut.edu.cn

Q. Yang
e-mail: yangql@whut.edu.cn

Z. Shi
e-mail: zqshi2016@whut.edu.cn

Q. Yang
Hainan Institute, Wuhan University of Technology, Sanya 572024, China

Z. Shi
School of Chemistry, Chemical Engineering and Life Sciences, Wuhan University of Technology, Wuhan 430070, China

Introduction

With the development of modern life, people's impact on the environment cannot be ignored. Organic dyes are the main pollutants in wastewater, and most of them are toxic and non-degradable (Shahid et al. 2021). The dyes enter the water will produce light

pollution, harm aquatic organisms and even cause human damage (Li et al. 2017; Tumolo et al. 2020). Therefore, it is very important to remove the dyes from wastewater even ultra-low concentration dyes. Today, there's many methods based on physics, chemistry and biology have been applied to dye removal technology. For example, coagulation (Shahid et al. 2021), flocculation (Ge and Li 2018; Liu et al. 2015), membrane separation (Zhao and Wang 2017), adsorption (Azari et al. 2020), ion exchange (Zhou et al. 2019), advanced oxidation method (Chowdhury et al. 2018), photocatalysis (Peng et al. 2017), biodegradation (Chen et al. 2020b), etc. Among them, dye adsorption technology (Qi et al. 2017) has attracted wide attention due to its high efficiency rate, low cost, and easy operation. Traditional adsorbents (Agartan et al. 2020) such as activated carbon not only cause secondary pollution, but also own low adsorption capacity, efficiency, and poor repeatability, which are difficult to meet the requirements of modern dye removal technology (Dehghani et al. 2017). Compared with traditional polymer materials, biomass materials have become a research hotspot in the field of dye adsorption due to their degradability and environmentally friendly properties (Li et al. 2015). Chitosan has hydroxyl and amino groups on the surface, it has good hydrophilicity and is used to remove pollutants (Fahimirad et al. 2021). Anderson et al. (Kriaa et al. 2011) studied chitosan heptadentate dinuclear ligand for the removal of low concentration metal ions, the results show that it has a selective removal effect on metal ions. The commonly used crosslinking agents for chitosan modification and grafting are glutaraldehyde and formaldehyde (Nagireddi et al. 2017), related studies have shown that it has side effects on aqueous solutions. Dai et al. (2021) used a one-step hydrothermal method to prepare a new type of magnetic lignin adsorbent to remove calcium ions and methylene blue from aqueous solutions, the adsorption capacities is 339.4 mg g^{-1} and 281.4 mg g^{-1}, respectively. This magnetic adsorbent has a good separation effect, but its adsorption capacity is limited (Ma et al. 2018). Ma et al. used a simple etching-sulfonation method to prepare a highly efficient and selective sulfonated lignin derivative adsorbent, showing that adsorbents with high negatively charged groups are excellent in the rapid removal performance of cationic dyes (Sarmah and Karak 2020). These works show that the modified biomass

macromolecules have functional groups such as sulfonic acid groups, amino groups, carboxyl groups, which is helpful for the application of adsorbents in the efficient removal of dyes.

Cellulose has a wide range of sources, degradability and biocompatibility (Sun et al. 2021). As the most abundant natural biomass material on earth, cellulose has the characteristics of low price and extensive renewability, and is an extremely attractive adsorption material (Xu et al. 2017). Cellulose macromolecules have the characteristics of high density of hydroxyl groups and hydrophilicity, which is conducive to the modification of functional groups (Liu et al. 2022; Nagarajan et al. 2021). Nanocellulose is a material with nanometer dimensions in one or more dimensions (Chen et al. 2020a). TEMPO oxidized cellulose nanofibers (TOCN) are nanomaterials with large aspect ratio and high specific surface area prepared by TEMPO oxidation method (Trache et al. 2020). The electrostatic repulsion between the carboxyl groups makes the nanocellulose present an interlaced network structure, which is conducive to the formation of a large specific surface area for TOCN (Oun et al. 2020). Nanocellulose particulate has good adsorption to cationic small molecules is 412 mg g^{-1} (Zhu et al. 2022). Nowadays, the cost of nanocelluloses is about 0.6 USD per dry kg, which is equal to the cost for the starting bleached wood pulps for papermaking (Akira Isogai 2020), with the development of more nanocellulose applications, this cost will be further reduced. Therefore, TOCN is a potential high-efficiency and low-cost adsorbent for the adsorption of cationic dyes.

In this study, nanocellulose gel beads with different carboxyl content were obtained by simple and rapid dropping solidification method and explored the influence of specific surface area and carboxyl content on the adsorption capacity of cationic dyes. The influence of all parameters related to adsorption performance such as specific surface area, contact time, pH and temperature of cationic dyes by nanofibrous beads was fully explored. The possible adsorption mechanism of nanofibrous beads was explored and interpretated by simulating kinetic model and adsorption isotherm model.

Experimental

Materials

Softwood bleached kraft pulp (SBKP, carboxyl content was 0.05 mmol/g, α-cellulose content of the pulp was 90%, and the rest was mostly xylan) was provided by Nippon Paper Industries (Tokyo, Japan). TEMPO was purchased from Sigma-aldrich Company of the United States, NaClO was purchased from Aladdin Biochemical Technology Co., LTD. NaBr, NaOH, CaCl$_2$, Methylene blue (MB), Ethanol were purchased from Sinopharm Group Chemical Reagent Co., Ltd. (China) and used without further purification.

Preparation of nanocellulose (TOCN) dispersion

TOCN were prepared form SBKP by purification, oxidation and homogenization (Saito et al. 2007; Wang et al. 2019). Purification was to removed heavy metal salt ions, including water washing and acid washing. After purification, cellulose pulp (2 g) was stirred with TEMPO (0.032 g) and NaBr (0.2 g) in deionized water (200 mL) at pH 10 and room temperature. In order to obtain TOCN with different carboxyl content, the amount of sodium hypochlorite was changed (2.5, 5, 7.5, 10 mmol/g-cellulose) and the time required for oxidation increased during the preparation process (Shi et al. 2015). Oxidation was stopped by adding ethanol, and 0.2 g NaBH$_4$ was added to reduce the aldehyde groups that were not completely oxidized at room temperature for 3 h. The TOCN was dispersed in aqueous medium, and placed in a high-pressure homogenizer (microchannel, 30 MPa) for the cellulose dispersion process to obtain a uniformly dispersed and transparent nanocellulose dispersion (0.55 wt%) under the action of high-pressure mechanical force. With the increase of the amount of sodium hypochlorite (2.5, 5, 7.5, 10 mmol/g-cellulose) this nanocellulose dispersion were named TOCN1, TOCN2, TOCN3, and TOCN4, respectively.

Preparation of nanocellulose beads with different carboxyl group content

100 mL of nanocellulose dispersion (0.55 wt%) was stirred for 30 min on a magnetic stirrer, and then was evacuated for 30 min to remove excess bubbles. 200 mL of 0.1 mol L^{-1} calcium chloride solution was prepared, and a 1 mL syringe was used to drop the nanocellulose dispersion into the calcium chloride solution. Subsequently, nanocellulose hydrogel beads (about 2 mm) quickly formed. Nanocellulose hydrogel beads prepared from dispersions with different carboxylate content were named TOCNB1, TOCNB2, TOCNB3, and TOCNB4, respectively. This dripping curing method allows the nanocellulose to contact the crosslinking agent in a large area. This gelation method is simple, rapid, and efficient. The higher the carboxyl content of nanocellulose beads, the faster the gelation.

Characterization

The morphologies of the surface of the different freeze-dried cellulose beads were observed by scanning electron microscope (SEM) (Hitachi S-4800, Japan) at 20 kV, and the internal pore size distribution and specific surface area analysis of the cellulose beads were performed by the Automatic specific surface area and porosity analyzer (TriStarIII3020, Micromeritics, American). Fourier transform infrared (FTIR) spectra of the dried microsphere sample were recorded by using a Nicolet FTIR spectrometer (Nicolet 6700, USA) over the range of 400–4000 cm^{-1}. Absorbance in the wavelength range of 300 to 800 nm of nanocellulose hydrogel beads were recorded by using ultraviolet-visible spectrophotometer (Lambda750S, America), the linear relation between absorbance and concentration was obtained. The surface potential of nanocellulose TOCN was measured by Zeta potentiometer at pH$=7$, $T=25$ °C environment. The formula $q_e = (C_0 - C_e)V/m$, $q_t = (C_0 - C_t)V/m$ and $RE\% = (C_0 - C_e)/C_0$ was used to calculate the equilibrium adsorption capacity and dye removal rate, In these formulas, q_e (mg g^{-1}) is the equilibrium adsorption capacity, C_0 (mg L^{-1}) is the initial concentration, C_e (mg L^{-1}) is the adsorption equilibrium concentration, C_t (mg L^{-1}) is the adsorption concentration at time t, V (L) is the volume of the dye solution, m (g) is the dry weight of the cellulose beads, and $RE\%$ is the dye removal rate. Unless otherwise specified the adsorption capacity general experimental conditions are pH$=7$, $T=25$ °C.

Results and discussion

### Structural morphology and surface analysis of nanocellulose beads

Figure 1 shows the surface morphology of nanocellulose hydrogel beads with different carboxyl group content, Fig. 1a–d are the SEM images at 20,000 magnification of nanocellulose with different carboxyl content. Nanocellulose beads present a smooth and flat surface and a porous fiber network structure. The adsorption capacity of the adsorbent is related to the pore size, it can be seen that the cellulose nanofibers in the nanocellulose beads form a stable three-dimensional network porous structure from Fig. 1e, f, and the pore size of the nanocellulose beads was is in the mesoporous range (several nanometers to several tens of nanometers). Relevant studies have shown that dye molecules hardly gather on the larger pore size of the adsorbent, and are mainly uniformly adsorbed on the small pores and mesoporous structure of the adsorbent (Qiao et al. 2021). This shows that the mesoporous structure of nanocellulose is beneficial to its application in the adsorption of small molecules (Gaduan et al. 2021).

Figure 2a is the nitrogen isotherm desorption curve of different nanocellulose beads. Under the same relative pressure, the adsorption capacity of TOCNB1, TOCNB2, TOCNB3, and TOCNB4 showed an increasing trend. The specific surface areas of TOCNB1, TOCNB2, TOCNB3, and TOCNB4 obtained by using the BET calculation model are 173 m^2/g, 246 m^2/g, 299 m^2/g, and 367 m^2/g, respectively, which shows that the increase in carboxylate content is beneficial to obtaining beads with a nanocellulose network structure with a larger specific surface area, the hydrogen bonds between nanocellulose molecules were weakened with the increase of carboxyl group content and specific surface area was increased. Figure 2b shows the pore size distribution curve of different nanocellulose beads. BET results showed that the pore diameters of nanocellulose beads were all concentrated between 5 and 15 nm, which belonged to the mesoporous structure, and the pore size of nanocellulose beads is relatively uniform. BET test shows that the specific surface area of nanocellulose beads was related to the content of carboxyl groups in nanocellulose. The increase in the content of carboxylate on the nanocellulose will promote the formation of a porous network structure with more pores and a larger specific surface area (Mishnaevsky et al. 2019). It indicates that, as a functional material with a controllable specific surface area, nanocellulose beads have much application potential.
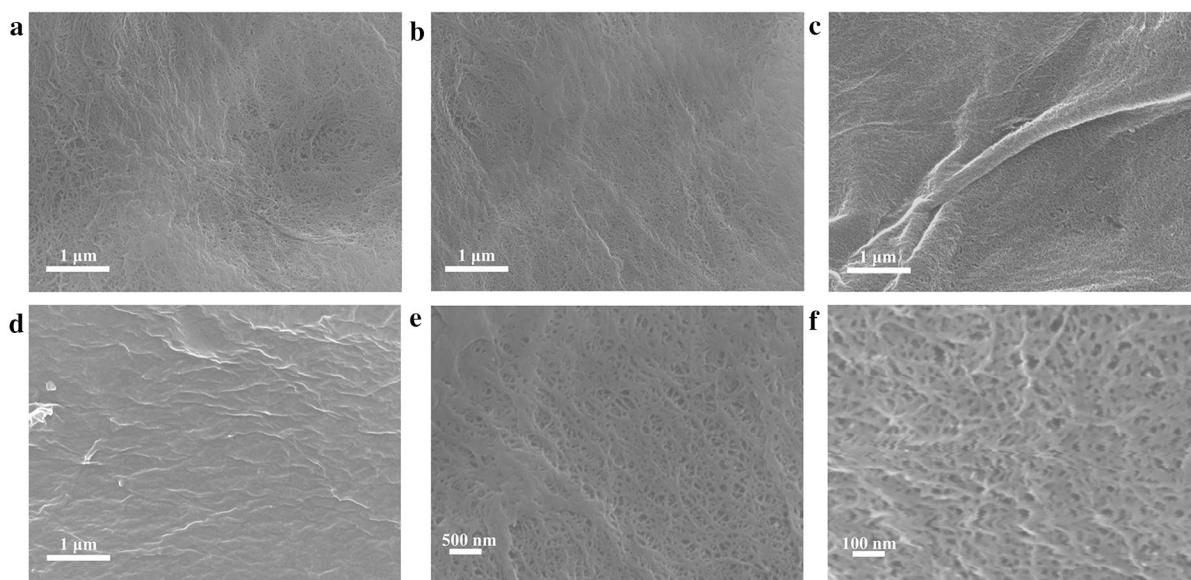
Fig. 1 SEM images **a** TOCNB1, **b** TOCNB2, **c** TOCNB3 and **d** TOCNB4. **e–f** amplified surface structure of TOCNB4.
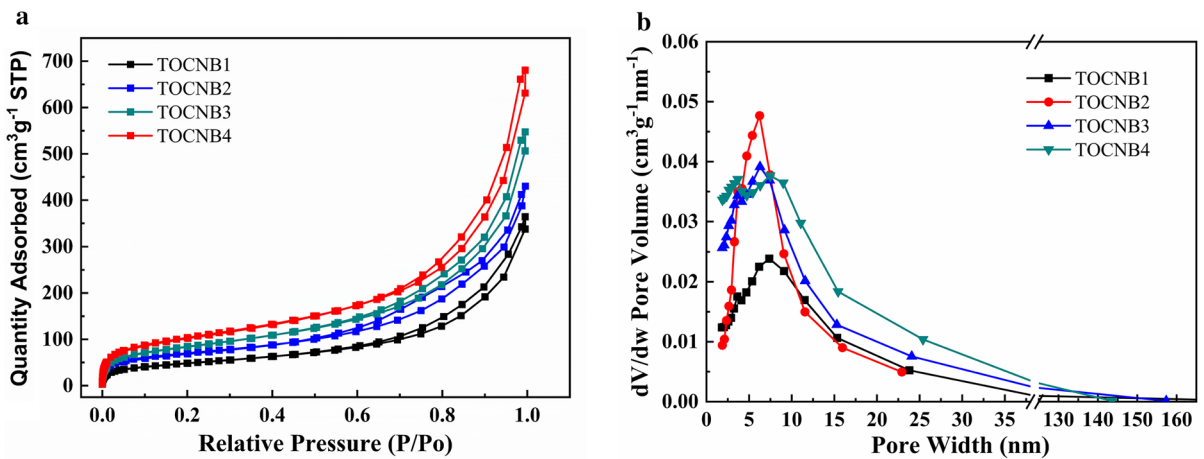
Fig. 2 **a** Curves of nitrogen isotherm adsorption-desorption of TOCNB. **b** Pore distribution curves of TOCNB.

Chemical structure analysis of nanocellulose beads

The FTIR spectra of TOCNB1, TOCNB2, TOCNB3 and TOCNB4 were shown in Fig. 3a. The peak at 3400 cm^{-1} was ascribed to the –OH stretching vibration in cellulose macromolecule, the peak at 2904 cm^{-1}, 1020 cm^{-1} and 1100 cm^{-1} was ascribed to the C–H, C–O and C–C stretching in cellulose macromolecule, respectively. The absorption peaks above were shown in all samples. The peak at 1614 cm^{-1} and 1424 cm^{-1} were represented for the asymmetric stretching and symmetrical stretching of –COO– in nanocellulose, respectively. The –COO– asymmetric stretching vibration peak of TOCN1, TOCN2, TOCN3 and TOCN4 at 1614 cm^{-1} showed a gradual increase, it indicates that the carboxyl group content increases. With the increasing of carboxyl content, the absorption band of TOCN at 3400 cm^{-1} shifts to a high wavenumber, which indicated that the hydrogen bonds between nanocellulose molecules were weakened with the increase of carboxyl group content. The mutual repulsion between the carboxylate ions will break the hydrogen bonds in the nanocellulose molecules, making the stretching vibration frequency of the hydroxyl groups on the nanocellulose molecules higher (Xue et al. 2017).
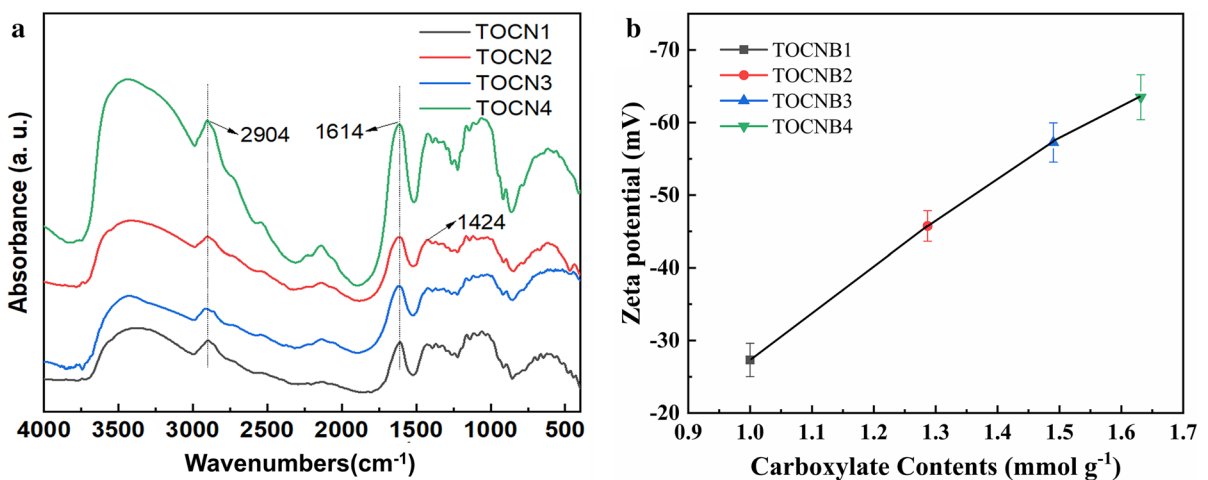

Fig. 3 **a** FT-IR spectra of TOCNB. **b** Zeta potential values of TOCNB.

The surface charge of the adsorbent is an important indicator of nanocellulose as a cationic adsorbent, the Zeta potential of TOCNB1, TOCNB2, TOCNB3 and TOCNB4 were shown in Fig. 3b, the potential values are -27 mV, -46 mV, -57 mV, and -63 mV, respectively. This shows that as the content of carboxyl groups increases, the negative surface charge of nanocellulose increases. This result not only confirmed the successful preparation of TOCN with different carboxyl group content, but also confirmed that nanocellulose that more carboxyl groups is expected to exhibit excellent adsorption performance in the application of high-efficiency cationic adsorbents.

Adsorption performance analysis of nanocellulose beads

To investigate the adsorption capacity of negatively charged nanocellulose beads for cationic dyes, methylene blue (MB) adsorption analysis was performed and the results were shown in Fig. 4. The initial concentration of MB is 5 mmol L^{-1}, as shown in Fig. 4a, different nanocellulose beads showed excellent adsorption capacity for cationic dye MB, which were 506 mg g^{-1}, 543 mg g^{-1}, 583 mg g^{-1}, 639 mg g^{-1} respectively, higher than 412 m g^{-1} (Zhu et al. 2022) and 281.4 mg g^{-1} (Dai et al. 2021). With the increase of carboxyl group content, the adsorption capacity of nanocellulose beads to MB was also enhanced. The concentration of dye was also one of the main factors
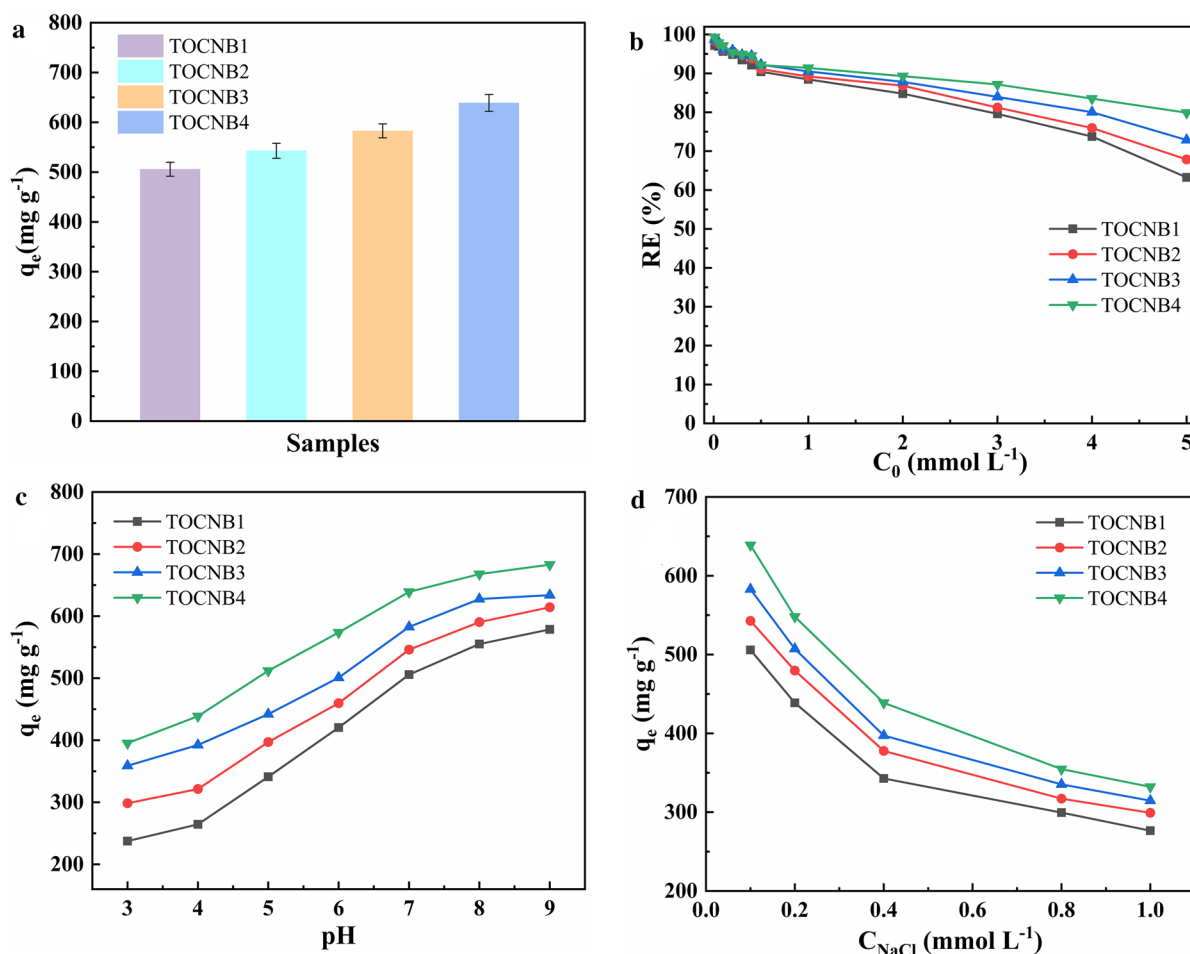
Fig. 4 a Adsorption capacities of TOCNB for MB. b Removal efficiency of TOCNB for MB. c Effects of pH on the adsorption of MB by TOCNB. d Effects of ions solutions on the adsorption of MB by TOCNB.

affecting adsorption. Investigating the adsorbent removal rate of dyes at different concentrations was helpful to understand the water purification capacity of the adsorbent and its application fields. MB solutions of different concentrations (0.01–5 mmol L^{-1}) were prepared to explore the dye removal rate of nanocellulose beads. As shown in Fig. 4b, at the low concentration (0.01–0.5 mmol L^{-1}) TOCNB owned an excellent removal effect on dyes, and the removal rate of nanocellulose beads with different carboxyl group content had no obvious difference, all of which were above 90%. With the increasing of dye concentration, the removal rate of dye increases with the increase of TOCNB carboxyl content. Among them, TOCNB4 still maintained a removal rate of 80% at concentration of 5 mmol L^{-1}. The high adsorption efficiency of TOCNB4 was still maintained at high concentrations, mainly due to the electrostatic interaction between carboxyl groups and dye molecules, and the aggregation of dyes at high concentrations (Qiao et al. 2021).
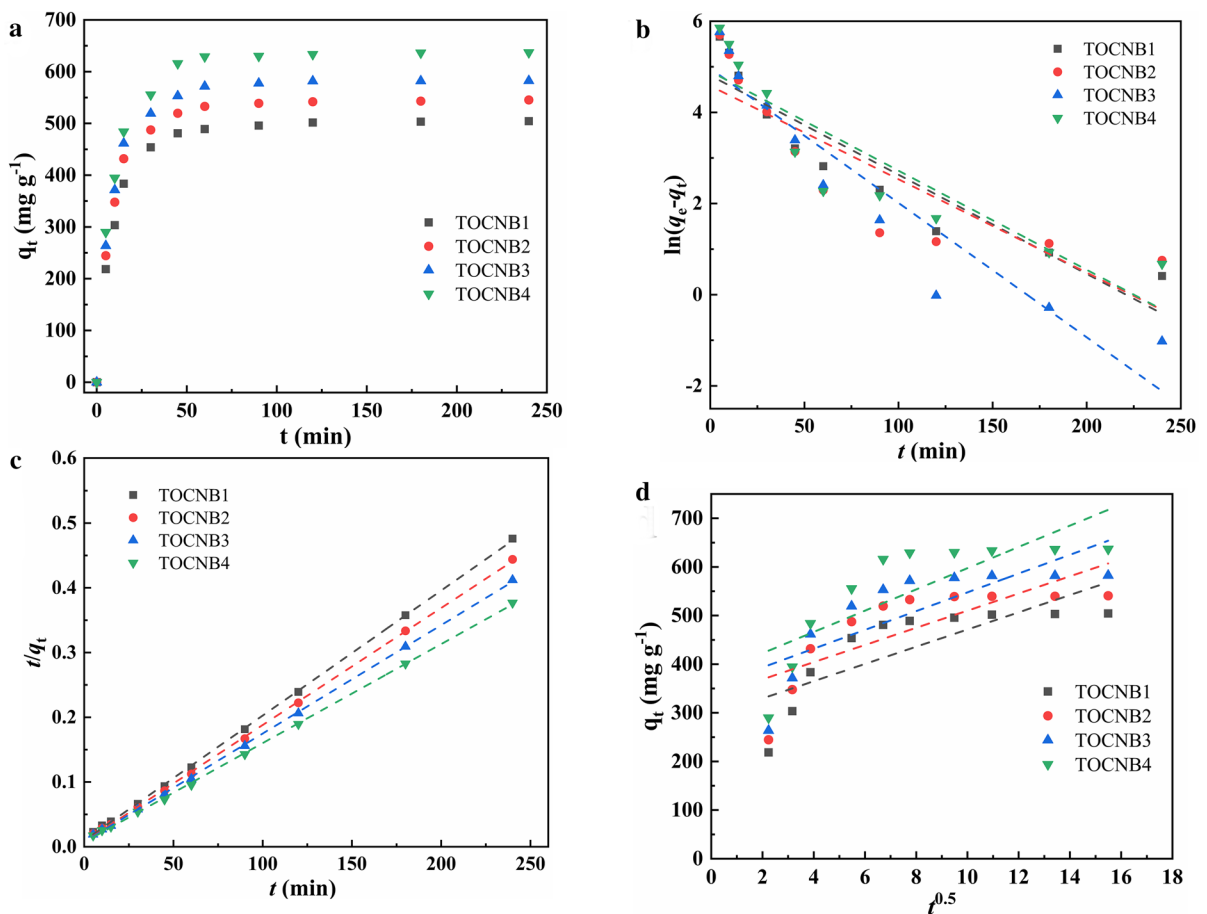
Because TOCNB was based on a cationic adsorbent under the action of static electricity, and the action of static electricity was significantly affected by the pH change of the solution. As shown in Fig. 4c, With the increase of the pH from 3 to 9 in the MB solution, the adsorption capacity of TOCNB on MB increased significantly. Among them, TOCNB1 increased from 237 to 538 mg g^{-1}, TOCNB2 increased from 298 to 614 mg g^{-1}, TOCNB3 increased from 360 to 633 mg g^{-1}, and TOCNB4 increased from 395 mg g^{-1} increased to 682 mg g^{-1}. In an acidic solution, the hydrogen ions in the solution and the dye molecules competed with each other, and the adsorption capacity of –COO$^-$ will deteriorate due to protonation. The increased alkalinity in the solution gradually weakened the adsorption competition from ions, which was conducive to enhancing the interaction between carboxylate ions and dye molecules, so that the adsorption capacity of TOCNB was significantly enhanced. This indicates that alkalinity can enhance the adsorption performance of cationic adsorbent (Luo et al. 2019). Figure 4d shows that with the increase of concentration of NaCl, the adsorption capacity of nanocellulose beads to dyes decreases. Relevant research has showed when there is electrostatic interaction between the dye and the adsorbent, the adsorption capacity of the dye will decrease with

the increase of the electrolyte concentration (Hong et al. 2018).

In the adsorption kinetics, the adsorption rate was an important indicator of the adsorption performance. As shown in, the adsorption capacity of nanocellulose beads rose rapidly in short time, especially in the first 20 min. This rapid adsorption effect was attributed to the electrostatic attraction between the negatively charged TOCNB and the positively charged MB dye. Subsequently, TOCNB reached adsorption equilibrium in 40–50 min. It can be obviously observed in the Fig. 5a that with the content of carboxyl groups increased, the adsorption rate of TOCNB increased significantly. It was worth noting that TOCNB4 owned abundant binding sites due to more carboxyl group content and larger specific surface area, so it took more time to reach adsorption equilibrium. It indicated that the carboxyl content and specific surface area of TOCNB were positively correlated with the dye adsorption capacity. This figure shows all TOCNB achieve adsorption equilibrium in 40–50 min. In order to further explore the adsorption kinetics of TOCNB with fast adsorption efficiency, pseudo-first-order kinetic model, pseudo-second-order kinetic model and intra-particle diffusion model were used to fit the adsorption data of TOCNB with time. The pseudo-first-order kinetic model was $ln(q_e - q_t) = ln q_e - k_1 t$, the pseudo-second-order kinetic model was $t/q_t = 1/k_2 q^2 e + t/q_e$, and the intra-particle diffusion model was $q_t = k_i t^{0.5} + C$. According to the corresponding fitted curve, the slope, intercept and corresponding dynamic parameter values were shown in Table 1. The curves of pseudo-first-order dynamic model were shown in Fig. 5b, c. The correlation coefficient (R^2) of TOCNB1, TOCN2, TOCN3 and TOCN4 were 0.85114,0.71711,0.87944 and 0.78287, respectively. The R^2 of curves that pseudo-second-order dynamic model of TOCNB1, TOCN2, TOCN3 and TOCN4 were 0.99965,0.99962,0.99967,0.99958. This showed that the pseudo-second-order kinetic model can better describe the adsorption mechanism of TOCNB. Saturated adsorption capacity (q_{max}) of TOCNB1, TOCN2, TOCN3 and TOCN4 calculated by pseudo-second-order kinetic model was closer to the experimental value. The pseudo-second-order kinetic model was based on the chemisorption hypothesis. Therefore, the main driving force for the adsorption of dyes by nanocellulose beads in the process of this experiment should be chemical

Table 1 Adsorption kinetic parameters of TOCNB adsorbent

	q_e-exp (mg g^{-1})	Pseudo-first-order $\ln(q_e - q_t) = \ln q_e - k_1 t$ q_e-cal (mg g^{-1}) k_1 (min^{-1})	Pseudo-second-order $t/q_t = 1/k_2 q_e^2 + t/q_e$ q_e-cal (mg g^{-1}) k_2 (min^{-1})	Intraparticle diffusion $q_t = k_3 t^{0.5} + C$ k_1 (min^{-1}) C
TOCNB1	505.76	121.62	518.13	568.61
		0.02177	0.00039	294.32
TOCNB2	542.79	92.01	552.49	607.14
		0.02049	0.00044	333.63
TOCNB3	582.75	142.94	595.24	653.87
		0.02949	0.00038	354.79
TOCNB4	638.89	131.49	653.59	717.54
		0.02177	0.00033	378.91

Fig. 5 **a** Effect of contact time on the adsorption of TOCNB to MB. **b** Curves of t-q_t based on pseudo-first-order kinetic model. **c** Curves of t-t/q_t based on pseudo-second-order kinetic model. **d** Curves of $t^{0.5}$-q_t based on intraparticle diffusion equation

interaction. The adsorption rate is limited by the availability of carboxyl groups. which were attributed to the high adsorption rate constant of TOCNB. Figure 5d simulated the intra-particle diffusion model

of TOCNB, the correlation coefficients of TOCNB1, TOCN2, TOCN3 and TOCN4 were 0.57389, 0.54391, 0.56586 and 0.58258, respectively. This indicated that particle diffusion within the particles was not the main mechanism of the TOCNB adsorption process. Increasing the diffusion time of dyes was not the only way to improve adsorption capacity. The adsorption process was controlled by both physical and chemical interactions. The adsorption process may also was affected by other influences, such as electromagnetic, ion exchange, hydrogen bonding, etc., which also affected the adsorption efficiency (Xu et al. 2021).

Adsorption isotherms of nanocellulose beads

The adsorption process between various adsorbents and small dye molecules can well described by adsorption isotherm. Therefore, the adsorption isotherm model of nanocellulose adsorbent was fitted. As shown in Fig. 6a, the nanocellulose bead adsorbent increased with the increase of adsorption equilibrium concentration, which was positively correlated with the initial concentration of dye. The increased of dye concentration increased the driving force of dye mass transfer from water to solid nanocellulose adsorbent, so as to provide more binding sites for MB and TOCNB to contact each other.
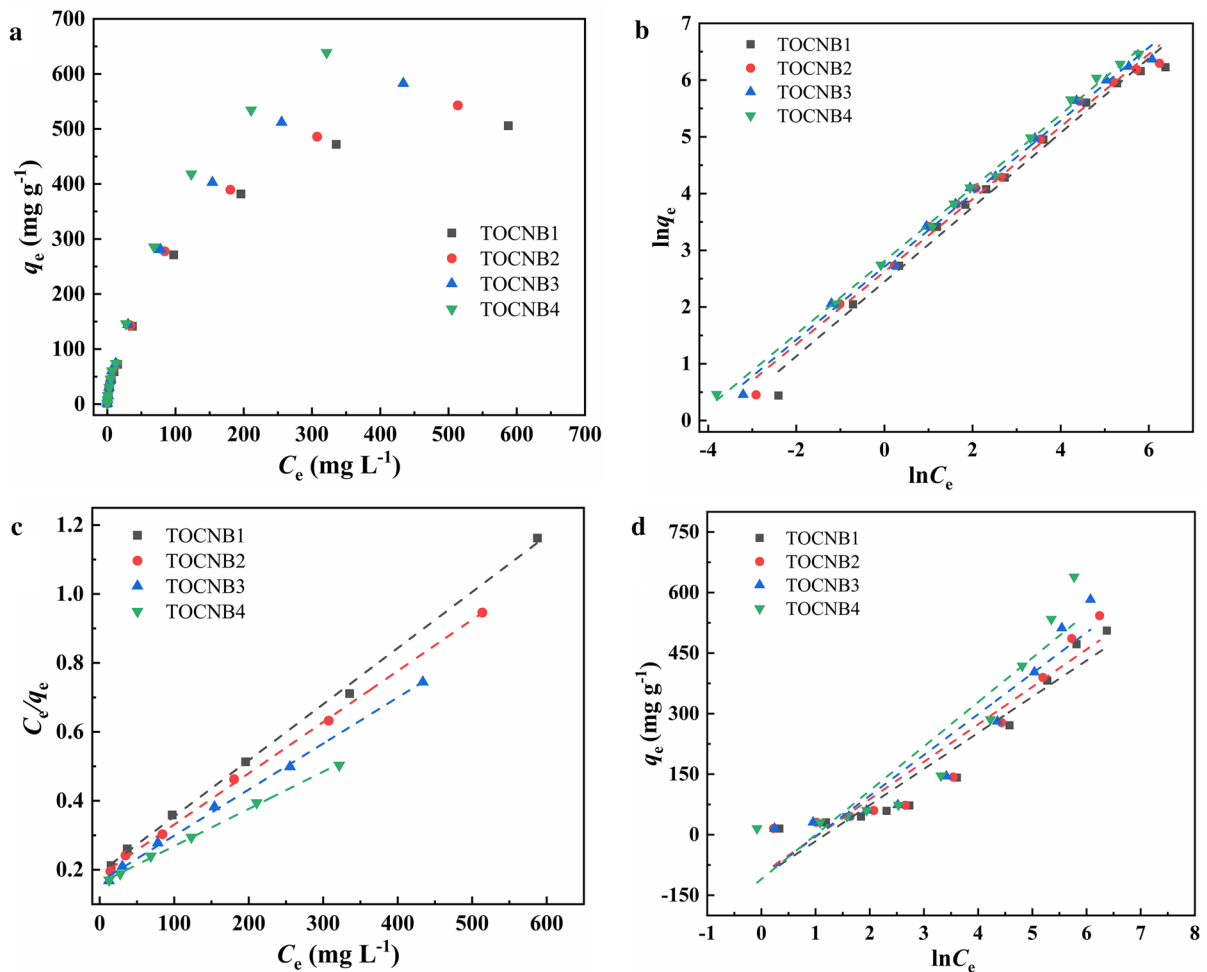
Fig. 6 a Adsorption isotherms for the adsorption of TOCNB1, TOCNB2, TOCNB3 and TOCNB4 towards MB. **b** Curves of $\ln C_e$-$\ln q_e$ based on pseudo-first-order kinetic model. **c** Curves of C_e-C_e/q_e based on pseudo-second-order kinetic model. **d** Curves of $\ln C_e$-q_e based on intraparticle diffusion equation

Three isothermal models were selected as follows, Freundlich isothermal model: $\ln q_e = \ln K_F + b_F \ln C_e$, Langmuir isothermal model: $C_e/q_e = C_e/q_m + 1/q_m K_L$, Temkin isothermal model: $q_e = B \ln K_T + B \ln C_e$, to explore the adsorption theory of TOCNB. The fitting results were shown in Fig. 6; Table 2. Langmuir isothermal model had the highest correlation coefficients: 0.99785, 0.99894, 0.99752 and 0.9984, which shown that TOCNB was more in line with this model. Langmuir isothermal model was based on the assumption that adsorption occurs at a specific homogeneous phase point and all homogeneous phase points are equal. Therefore, adsorption of MB based on TOCNB occurs at a specific homogeneous phase
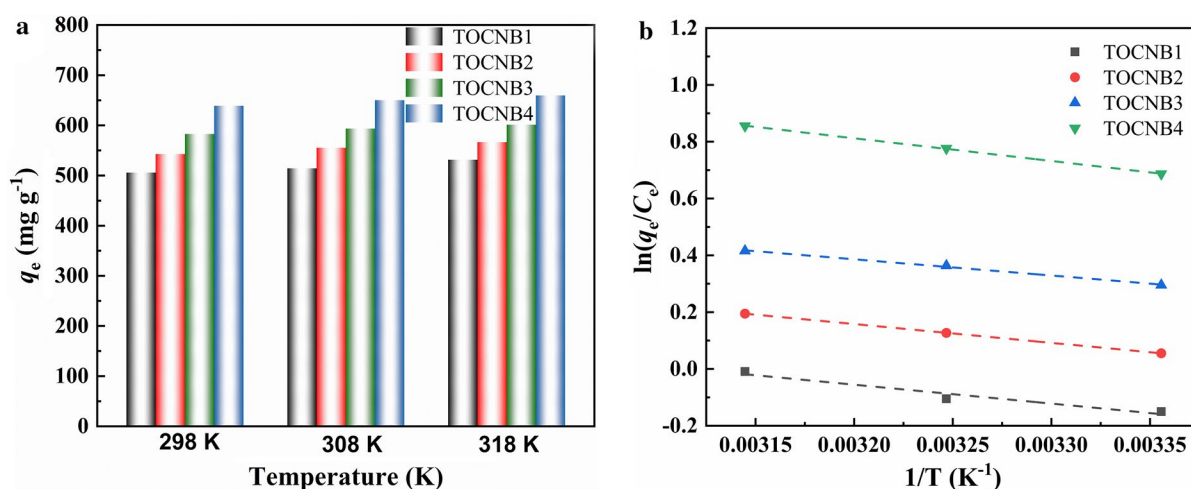
point. The adsorption process of TOCNB to MB is monolayer and uniform (Hokkanen et al. 2013).

Effect of temperature on adsorption properties of nanocellulose beads

Generally, the temperature has a certain effect on the adsorption performance. The thermodynamic behavior of the adsorbent was studied by using the change of the adsorption capacity of the adsorbent at different temperatures. Thermodynamic parameters included free energy change, enthalpy change and entropy change. These parameters were used to evaluate the adsorption behavior of TOCNB. As shown in Fig. 7a, the adsorption capacity of TOCNB for MB increased

Table 2 Adsorption isotherm parameters for the adsorption of TOCNB adsorbent

	q_e-exp (mg g^{-1})	Freundlich $\ln q_e = \ln K_F + b_F \ln C_e$ k_F (mg g^{-1}) b_F	Langmuir $C_e/q_e = C_e/q_m + 1/q_m K_L$ q_m (mg g^{-1}) k_L (L mg^{-1})	Temkin $q_e = B \ln K_T + B \ln C_e$ k_T (L mg^{-1}) B (KJ^{-2} mol^{-2})
TOCNB1	505.76	11.547	613.49	0.3078
		0.65662	117.76	89.52052
TOCNB2	542.79	13.768	671.14	0.3496
		0.63942	123.27	92.78642
TOCNB3	582.75	15.052	746.27	0.3526
		0.64402	123.60	101.02872
TOCNB4	638.89	16.688	925.93	0.3670
		0.64514	148.96	109.65589

Fig. 7 **a** Effect of temperature on the adsorption of TOCNB1, TOCNB2, TOCNB3 and TOCNB4 towards MB. **b** Curves of $1/T$-$\ln(q_{e-}C_e)$ based on van't Hoff equation

with the increase of temperature. The van Hoff equation: $\ln(q_e/C_e) = \Delta S/R - \Delta H/RT$, q_e (mg g^{-1}) was the equilibrium adsorption capacity of TOCNB, C_e (mg L^{-1}) was the equilibrium concentration of dyes, T (K) was the specified temperature, and R (8.314 J mol^{-1}k^{-1}) was the ideal gas constant. The curve obtained by fitting was shown in Fig. 7b, The correlation coefficients of TOCNB1, TOCNB2, TOCNB3, and TOCNB4 were 0.95095, 0.9999, 0.99335, and 0.99932, respectively. Free energy change, enthalpy change and entropy change were calculated. As shown in Table 3, the adsorption data of TOCNB in temperature was well fitted by the van Hoof equation, the enthalpy change and entropy change of TOCNB were both positive, and the free energy change was negative, indicated that the adsorption process of TOCNB to MB was endothermic, also spontaneous. The adsorption process shown that the adsorption capacity increased with the increase of temperature, and higher temperature was beneficial to the progress of adsorption. This was consistent with our experimental results.
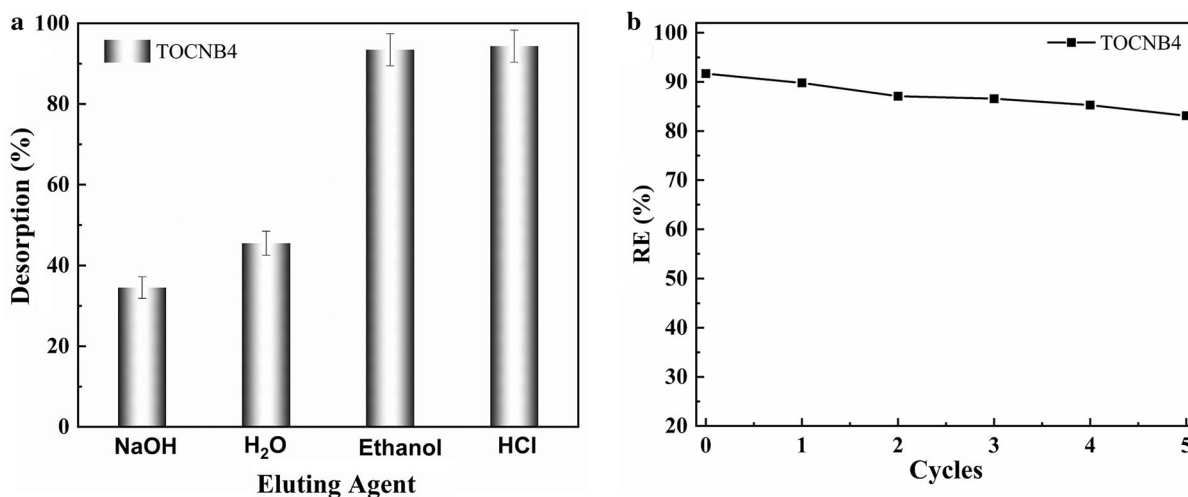
Analysis of desorption performance of nanocellulose beads

In the practical application of adsorbents, desorption capacity and regeneration capacity were the key factors to evaluate the performance of adsorbents, these reflected the ability of the adsorbent to be reused. Different solutions such as sodium hydroxide solution (1 mol L^{-1}), deionized water, ethanol and hydrochloric acid solution (1 mol L^{-1}) were used as eluents to study the desorption performance of TOCNB adsorbent. The desorption efficiency obtained by desorbing TOCNB adsorbed MB was shown in Fig. 8a. The desorption efficiencies after desorption with HCl and ethanol were as high as 93% and 94%, with deionized water and sodium hydroxide solution were 45% and 34%, which meant that TOCNB can be desorbed by

Table 3 Thermodynamic parameters for the adsorption of TOCNB adsorbent

	ΔH (kJ mol^{-1})	ΔS (J mol^{-1} k^{-1})	ΔG (kJ mol^{-1}) 298 K, 308 K, 318 K
TOCNB1	5.53	17.24	− 5.13, − 5.30, − 5.48
TOCNB2	5.50	18.93	− 5.64, − 5.82, − 6.01
TOCNB3	4.75	18.40	− 5.48, − 5.66, − 5.85
TOCNB4	6.65	28.04	− 8.35, − 8.63, − 8.91

Fig. 8 a Desorption performance of TOCNB4 after washing with diverse eluting agents. **b** Five cycles of desorption-adsorption with TOCNB4 towards MB.

HCl or ethanol solution to obtain a cationic adsorbent that can be regenerated for multiple times. HCl was used as eluent to wash TOCNB4, the removal rate of 1 mmol L^{-1} MB solution for five cycles was shown in Fig. 8b. Obviously, TOCNB4 had a high removal rate of 83% for MB after five cycles. This verified that TOCNB was a high-efficiency adsorbent with good regenerable cycle performance and reusability.

Conclusion

In this work, TOCNB were prepared by a simple dropping method, and changing the content of sodium hypochlorite in the TEMPO oxidation method to control the carboxyl group content of nanocellulose. TOCNB shows a three-dimensional network porous structure, which is composed of interwoven cellulose nanofibers. TOCNB has large specific surface area and uniform pore size distribution, which concentrated at 10–15 nm, the pores are mainly mesoporous structure. The surface potential and adsorption results show that the more carboxyl group content, the more negative the potential value, and the better adsorption capacity for MB. Under alkaline conditions, TOCNB has stronger adsorption capacity for MB, the adsorption kinetics of TOCNB fit a second-order model, and the main driving force was chemical interaction. The adsorption isotherm model of TOCNB is more in line with the Langmuir isotherm model, the adsorption process is homogeneous and monolayer, and the saturation adsorption value of TOCNB is as high as 925.93 mg g^{-1}. The effect of temperature on adsorption shows the process of MB adsorption by TOCNB is endothermic and spontaneous, increasing the temperature is beneficial to adsorption. The results of desorption experiments showed that TOCNB still had a high removal rate of 83% for MB after five cycles of TOCNB4. This verifies that TOCNB is a high-efficiency adsorbent with good regenerable cycle performance and reusability and has great application prospects in water pollution control.

Author contributions JX: Writing—original draft, Investigation, Methodology, Formal analysis. EZ: Writing—review and editing, Validation, Investigation, Data curation, Visualization. HZ: Investigation. DL: Investigation. HC: Conceptualization, Writing—review and editing. CX: Writing—review and editing. QY: Investigation, Writing—review and editing. ZS: Conceptualization, methodology, project administration, Writing—review and editing, supervision.

Data availability The datasets used and/or analysis during the current study are available from the corresponding author on reasonable request.

Declarations

Conflict of interest The authors have no relevant financial or non-financial interests to disclose.

Consent for publication All authors were informed and agreed to publish in cellulose.

References

Agartan L, Hantanasirisakul K, Buczek S, Akuzum B, Mahmoud KA, Anasori B, Gogotsi Y, Kumbur EC (2020) Influence of operating conditions on the desalination performance of a symmetric pre-conditioned $Ti_3C_2T_x$-MXene membrane capacitive deionization system. Desalination. https://doi.org/10.1016/j.desal.2019.114267

Akira Isogai (2020) Emerging Nanocellulose Technologies: recent developments. ADV MATER 33(28):2000630. https://doi.org/10.1002/adma.202000630

Azari A, Nabizadeh R, Nasseri S, Mahvi AH, Mesdaghinia AR (2020) Comprehensive systematic review and meta-analysis of dyes adsorption by carbon-based adsorbent materials: classification and analysis of last decade studies. Chemosphere 250:126238. https://doi.org/10.1016/j.chemosphere.2020.126238

Chen C, Kuang Y, Zhu S, Burgert I, Keplinger T, Gong A, Li T, Berglund L, Eichhorn SJ, Hu L (2020a) Structure–property–function relationships of natural and engineered wood. Nat Rev Mater 5(9):642–666. https://doi.org/10.1038/s41578-020-0195-z

Chen R, Cai J, Li Q, Wei X, Min H, Yong Q (2020) Coadsorption behaviors and mechanisms of pb (ii) and methylene blue onto a biodegradable multi-functional adsorbent with temperature-tunable selectivity. RSC Adv 10(59):35636–35645. https://doi.org/10.1039/d0ra07139k

Chowdhury M, Hossain M, Azad M, Islam M, Dewan M (2018) Photocatalytic degradation of methyl orange under UV using ZnO as catalyst. Int J Engine Res 9. https://doi.org/10.14299/ijser.2018.06

Dai K, Zhao G, Kou J, Wang Z, Zhang J, Wu J, Yang P, Li M, Tang C, Zhuang W et al (2021) Magnetic mesoporous sodium citrate modified lignin for improved adsorption of calcium ions and methylene blue from aqueous solution. J Environ Chem Eng 9(2):105180. https://doi.org/10.1016/j.jece.2021.105180

Dehghani MH, Dehghan A, Najafpoor A (2017) Removing reactive Red 120 and 196 using chitosan/zeolite composite from aqueous solutions: kinetics, isotherms, and process optimization. J Ind Eng Chem 51:185–195. https://doi.org/10.1016/j.jiec.2017.03.001

Fahimirad S, Abtahi H, Satei P, Ghaznavi-Rad E, Moslehi M, Ganji A (2021) Wound healing performance of PCL/chitosan based electrospun nanofiber electrosprayed with curcumin loaded chitosan nanoparticles. Carbohydr Polym. https://doi.org/10.1016/j.carbpol.2021.117640

Gaduan AN, Solhi L, Kontturi E, Lee K-Y (2021) From micro to nano: polypropylene composites reinforced with TEMPO-oxidised cellulose of different fibre widths. Cellulose 28(5):2947–2963. https://doi.org/10.1007/s10570-020-03635-3

Ge Y, Li Z (2018) Application of lignin and its derivatives in adsorption of heavy metal Ions in water: a review. ACS Sustain Chem Eng 6(5):7181–7192. https://doi.org/10.1021/acssuschemeng.8b01345

Hokkanen S, Repo E, Sillanpaa M (2013) Removal of heavy metals from aqueous solutions by succinic anhydride modified mercerized nanocellulose. Chem Eng J 223:40–47. https://doi.org/10.1016/j.cej.2013.02.054

Hong HJ, Lim JS, Hwang JY, Kim M, Jeong HS, Park MS (2018) Carboxymethlyated cellulose nanofibrils (CMC-NFs) embedded in polyurethane foam as a modular adsorbent of heavy metal ions. Carbohydr Polym 195:136–142. https://doi.org/10.1016/j.carbpol.2018.04.081

Kriaa A, Hamdi N, Srasra E (2011) Adsorption studies of methylene blue dye on tunisian activated lignin. Russ J Phys Chem A 85(2):279–287. https://doi.org/10.1134/S0036024411020191

Li J, Su Z, Xu H, Ma X, Yin J, Jiang X (2015) Supramolecular networks of hyperbranched poly (ether amine) (hPEA) nanogel/chitosan (CS) for the selective adsorption and separation of guest molecules. Macromolecules 48(7):2022–2029. https://doi.org/10.1021/ma502607p

Li R, Gao B, Guo K, Yue Q, Zheng H, Wang Y (2017) Effects of papermaking sludge-based polymer on coagulation behavior in the disperse and reactive dyes wastewater treatment. Bioresour Technol 240:59–67. https://doi.org/10.1016/j.biortech.2017.02.088

Liu L, Gao ZY, Su XP, Chen X, Jiang L, Yao JM (2015) Adsorption removal of dyes from single and binary solutions using a cellulose-based bioadsorbent. ACS Sustain Chem Eng 3(3):432–442. https://doi.org/10.1021/sc500848m

Liu D, Gao Y, Song Y, Zhu H, Zhang L, Xie Y, Shi H, Shi Z, Yang Q, Xiong C (2022) Highly sensitive multifunctional electronic skin based on nanocellulose/mxene composite films with good electromagnetic shielding biocompatible antibacterial properties. Biomacromolecules 23(1):182–195. https://doi.org/10.1021/acs.biomac.1c01203

Luo Y, Liu M, Chen Y, Wang T, Zhang W (2019) Preparation and regeneration of iron-modified nanofibres for low-concentration phosphorus-containing wastewater treatment. R Soc Open Sci. https://doi.org/10.1098/rsos.190764

Ma Y, Zheng D, Mo Z, Dong R, Qiu X (2018) Magnetic lignin-based carbon nanoparticles and the adsorption for removal of methyl orange. Colloids Surf A 559:226–234. https://doi.org/10.1016/j.colsurfa.2018.09.054

Mishnaevsky L Jr, Mikkelsen LP, Gaduan AN, Lee KY, Madsen B (2019) Nanocellulose reinforced polymer composites: computational analysis of structure–mechanical properties relationships. Compos Struct. https://doi.org/10.1016/j.compstruct.2019.111024

Nagarajan KJ, Ramanujam NR, Sanjay MR, Siengchin S, Surya Rajan B, Sathick Basha K, Madhu P, Raghav GR (2021) A comprehensive review on cellulose nanocrystals and cellulose nanofibers: pretreatment, preparation, and characterization. Polym Compos 42(4):1588–1630. https://doi.org/10.1002/pc.25929

Nagireddi S, Katiyar V, Uppaluri R (2017) Pd (II) adsorption characteristics of glutaraldehyde cross-linked chitosan copolymer resin. Int J Biol Macromol 94:7284. https://doi.org/10.1016/j.ijbiomac.2016.09.088

Oun AA, Shankar S, Rhim JW (2020) Multifunctional nanocellulose/metal and metal oxide nanoparticle hybrid nanomaterials. Crit Rev Food Sci Nutr 60(3):435–460. https://doi.org/10.1080/10408398.2018.1536966

Peng Y, Wang KK, Liu T, Xu J, Xu BG (2017) Synthesis of one-dimensional Bi_2O_3–$Bi_2O_{2.33}$ heterojunctions with high interface quality for enhanced visible light photocatalysis in degradation of high-concentration phenol and MO dyes. Appl Catal B 203:946–954. https://doi.org/10.1016/j.apcatb.2016.11.011

Qi F, Yan Y, Lamb D, Naidu R, Bolan NS, Liu Y, Ok YS, Donne SW, Semple KT (2017) Thermal stability of biochar and its effects on cadmium sorption capacity. Bioresour Technol 246:48–56. https://doi.org/10.1016/j.biortech.2017.07.033

Qiao A, Cui M, Huang R, Ding G, Qi W, He Z, Klemes JJ, Su R (2021) Advances in nanocellulose-based materials as adsorbents of heavy metals and dyes. Carbohydr Polym. https://doi.org/10.1016/j.carbpol.2021.118471

Saito T, Kimura S, Nishiyama Y, Isogai A (2007) Cellulose nanofibers prepared by TEMPO-mediated oxidation of native cellulose. Biomacromolecules 8(8):2485–2491. https://doi.org/10.1021/bm0703970

Sarmah D, Karak N (2020) Double network hydrophobic starch based amphoteric hydrogel as an effective adsorbent for both cationic and anionic dyes. Carbohydr Polym 242:116320. https://doi.org/10.1016/j.carbpol.2020.116320

Shahid S, Sultana T, Sultana S, Hussain B, Irfan M, Al-Ghanim KA, Misned FA, Mahboob S (2021) Histopathological alterations in gills, liver, kidney and muscles of ictalurus punctatus collected from pollutes areas of river. Braz J Biol 81(3):814–821. https://doi.org/10.1590/1519-6984.234266

Shi Z, Yang Q, Ono Y, Funahashi R, Saito T, Isogai A (2015) Creation of a new material stream from japanese cedar resources to cellulose nanofibrils. React Funct Polym 95:19–24. https://doi.org/10.1016/j.reactfunctpolym.2015.08.005

Sun Y, Chu Y, Wu W, Xiao H (2021) Nanocellulose-based lightweight porous materials: a review. Carbohydr Polym 255:117489. https://doi.org/10.1016/j.carbpol.2020.117489

Trache D, Tarchoun AF, Derradji M, Hamidon TS, Masruchin N, Brosse N, Hussin MH (2020) Nanocellulose: from fundamentals to advanced applications. Front Chem. https://doi.org/10.3389/fchem.2020.00392

Tumolo M, Ancona V, De Paola D, Losacco D, Campanale C, Massarelli C, Uricchio VF (2020) Chromium pollution in european water, sources, health risk, and remediation strategies: an overview. ACS Sustain Chem Eng. https://doi.org/10.3390/ijerph17155438

Wang H, Zuo M, Ding N, Yan G, Zeng X, Tang X, Sun Y, Lei T, Lin L (2019) Preparation of nanocellulose with high-pressure homogenization from pretreated biomass with cooking with active oxygen and solid alkali. ACS Sustain Chem Eng 7(10):9378–9386. https://doi.org/10.1021/acssuschemeng.9b00582

Xu QH, Wang YL, Jin LQ, Wang Y, Qin MH (2017) Adsorption of Cu (II), pb (II) and cr (VI) from aqueous solutions using black wattle tannin-immobilized nanocellulose. J Hazard Mater 339:91–99. https://doi.org/10.1016/j.jhazmat.2017.06.005

Xu X, Ouyang X, Yang L (2021) Adsorption of pb(II) from aqueous solutions using crosslinked carboxylated chitosan/carboxylated nanocellulose hydrogel beads. J Mol Liq. https://doi.org/10.1016/j.molliq.2020.114523

Xue Y, Mou Z, Xiao H (2017) Nanocellulose as a sustain biomass material: structure, properties, present status and future prospects in biomedical applications. Nanoscale 9(39):14758–14781. https://doi.org/10.1039/C7NR04994C

Zhao S, Wang Z (2017) A loose nano-filtration membrane prepared by coating HPAN UF membrane with modified PEI for dye reuse and desalination. J Membr Sci 524:214–224. https://doi.org/10.1016/j.memsci.2016.11.035

Zhou Y, Lu J, Zhou Y, Liu Y (2019) Recent advances for dyes removal using novel adsorbents: a review. Environ Pollut 252:352–365. https://doi.org/10.1016/j.envpol.2019.05.072

Zhu H, Zhu E, Xie Y, Liu D, Hu Y, Shi Z, Xiong C, Yang Q (2022) Hydrangea-like nanocellulose microspheres with high dye adsorption and drug encapsulation prepared by emulsion method. Carbohydr polym 296:119947. https://doi.org/10.1016/j.carbpol.2022.119947